Femtosecond Vibrational Dynamics of Self-Trapping in a Quasi-One-Dimensional System

S. L. Dexheimer* and A. D. Van Pelt
Department of Physics, Washington State University, Pullman, Washington 99164-2814

J. A. Brozik† and B. I. Swanson
Chemical Science and Technology Division, Los Alamos National Laboratory, Los Alamos, New Mexico 87545
(Received 3 September 1999)

We have directly time resolved the lattice motions associated with the formation of the self-trapped exciton in the quasi-one-dimensional system $[Pt(en)_2][Pt(en)_2Br_2] \cdot (PF_6)_4$ (en = ethylene-diamine, $C_2H_8N_2$), using femtosecond impulsive excitation techniques. A strongly damped, low-frequency wave packet modulation at ~ 110 cm^{-1} accompanies the formation of the self-trapped exciton on a ~ 200 fs time scale following excitation of the intervalence charge-transfer transition. Coherent oscillations at the ground state vibrational frequency and its harmonics are also detected.

PACS numbers: 71.35.Aa, 78.47.+p, 78.55.Hx

The dynamics of localized electronic states play an important role in determining the properties of many electronic materials. The formation of localized photoinduced states in a material can dramatically alter its optical characteristics as well as its transport properties. Examples include metastable defects in amorphous silicon, *DX* centers in GaAs and related semiconductors, color centers in alkali halide crystals, excitons in molecular complexes, and the self-trapped electronic excitations in low-dimensional materials [1,2]. A dominant factor in the dynamics of these localized states is the interplay between their electronic and vibrational degrees of freedom. Low-dimensional materials, and especially quasi-one-dimensional materials are ideal systems for studying these electron-lattice interactions: the reduced dimensionality can lead to strong electron-phonon interactions, and the linear structure of the materials simplifies the dynamical configuration space, in that the dominant motion is expected to occur along the linear axis.

In this work, we have directly time resolved the vibrational motions associated with the formation of the self-trapped exciton (STE) in a quasi-one-dimensional system. The experiments were carried out using femtosecond impulsive excitation techniques on the halogen-bridged mixed-valence linear chain complex $[Pt(en)_2][Pt(en)_2Br_2] \cdot (PF_6)_4$ (en = ethylenediamine, $C_2H_8N_2$), also abbreviated as PtBr(en). The essential elements of the linear structure of this complex can be represented as $\ldots -Br^- - Pt^{(3+\delta)} - Br^- - Pt^{(3-\delta)} - Br^- - \ldots$, which shows both the periodic charge disproportionation (or mixed-valence character) and the periodic bond length distortion (or Peierls distortion) characteristic of its charge density wave ground state. The ethylenediamine ligands fill the transverse bonding sites on the octahedrally coordinated metal ions, and the PF_6 counterions serve to balance the overall charge in the crystal structure, as well as to spatially separate the chains so that they experience minimal interchain interaction.

The dominant feature in the optical absorption spectrum of the metal-halide complexes is an intense optical intervalence charge transfer (IVCT) transition, highly polarized along the chain axis, in which electron density is transferred between inequivalent metal sites. Since the equilibrium metal-halide bond lengths depend on the charge distribution about the metal ions, the intervalence charge transfer transition is strongly coupled to the metal-halide vibrations, and the IVCT optical absorption band is exceptionally broad. For PtBr(en) at room temperature, the onset of this absorption band falls at approximately 800 nm, and its peak falls at approximately 550 nm. The vibrational properties of metal-halide chain complexes are well characterized by Raman and far-infrared spectroscopies [3]. The vibrational spectra of the complexes have been interpreted in detail, and reveal strong modes involving motions along the chain axis. In PtBr complexes, these include a Raman-active symmetric stretch of the Br ions about the Pt ions at a frequency of ~ 180 cm^{-1}, an infrared-active asymmetric stretch at ~ 240 cm^{-1}, and a weak, lower frequency infrared-active mode at ~ 95 cm^{-1}. Because of the symmetries of the modes, only the symmetric stretch mode is coupled to the IVCT optical transition.

In the linear chain complexes, as in other quasi-one-dimensional systems, the strong electron-phonon coupling leads to the formation of localized excitations such as self-trapped excitons, solitons, and polarons. In the case of the metal-halide complexes, excitation of the IVCT band creates a highly nonequilibrium lattice configuration, and subsequent lattice relaxation and charge transfer processes lead to the evolution the excitations. Theoretical work based on Peierls-Hubbard models has postulated the formation of a self-trapped exciton state following photoexcitation and has predicted its decay into solitons, polarons, and bipolarons [4].

Since self-trapping in an ideal one-dimensional system is theoretically predicted to be a barrierless process (in contrast to three-dimensional systems where, in general, there is an adiabatic potential barrier between the free and self-trapped states) [2], the formation time for the self-trapped exciton is expected to be short. Previous experimental

work on metal-halide complexes similar to that used in the current study indicates that the dynamics are rapid: luminescence measurements on PtCl complexes indicate a large Stokes shift as well as subpicosecond to picosecond luminescence lifetimes that have been attributed to cooling and decay of the self-trapped exciton state [5]. In addition, transient absorption measurements have revealed a redshifted induced absorbance assigned to the self-trapped exciton state that decays on a picosecond time scale [6]. The initial relaxation processes leading to the formation of the self-trapped exciton are thought to occur on a femtosecond time scale, consistent with the idea that the chain-axis vibrational motions directly drive this process.

The measurements in this study were carried out using a femtosecond pump-probe technique, in which an ultrashort pump pulse excites the sample and a time-delayed probe pulse measures the resulting change in transmittance as a function of pump-probe delay. An interesting limiting case of the optical pump-probe technique results when the light pulses are short compared to the periods of the characteristic vibrations of the material. In this case, the vibrational modes coupled to the electronic transition are impulsively excited, creating vibrational wave packets that consist of coherent superpositions of vibrational states [7]. These nonstationary vibrational wave packets, which can be formed on both the ground and excited potential energy surfaces, oscillate at the characteristic vibrational frequencies of the material and are observable as a time-dependent modulation of the differential transmittance signal. Impulsive excitation is especially useful for studying vibrational dynamics associated with electronic excitation: only those vibrations that are coupled to the electronic transition are excited, and the evolution of the wave packet oscillations directly reflects the nuclear dynamics, providing a means to observe the role of specific vibrational motions in fast photoinduced processes. Most importantly, impulsive excitation measurements can be sensitive to excited state vibrations, in contrast to cw Raman spectroscopy, which detects only ground state vibrational frequencies.

In the experiments reported here, we have excited the IVCT transition near the band gap using light pulses 35 fs in duration, short compared to the fundamental Raman-active chain-axis vibrational mode (frequency ~ 180 cm^{-1}, period ~ 185 fs). The pulse spectrum is centered at 800 nm, with a FWHM of ~ 30 nm. The pulses were generated by an amplified Ti:sapphire laser system operating at a repetition rate of 1 kHz, thereby minimizing potential artifacts due to multiple excitation effects. Transient absorption measurements were carried out using probe pulses derived either by splitting off part of the pump pulse (degenerate pump probe) or by generating a broadband femtosecond continuum in a 2-mm-thick sapphire plate. The near-infrared part of the continuum was compressed using a fused silica prism dispersive delay line, giving a cross-correlation width of ~ 50 fs over the detected wavelength ranges. Wavelength resolution was achieved in the transient absorption measurements by spectrally filtering the probe pulse after it had passed through the sample. The experimental samples were single crystals of $[Pt(en)_2][Pt(en)_2Br_2] \cdot (PF_6)_4$ of good optical quality, oriented with the chain axis parallel to the polarization of the pump and probe pulses. Recent advances in the synthesis of the metal-halide complexes have resulted in the production of materials that are largely free of defects and that are resistant to photoinduced damage [8].

The time-resolved response following impulsive excitation into the IVCT band is shown in Fig. 1(a). These measurements were taken in the continuum-probe configuration at a series of detection wavelengths extending well beyond the pump pulse spectrum. The data reveal the formation of an induced absorbance, redshifted relative to the ground state absorption, that has been assigned to the self-trapped exciton state. The signal is strongly modulated by vibrational wave packet oscillations that correspond directly to lattice motions initiated by the impulsive electronic excitation. Strong oscillatory components are evident at the frequency of the Raman-active symmetric stretch chain mode, as well as at a lower frequency that is seen to create a beat pattern at short times that varies with detection wavelength. The Fourier power spectra of the oscillatory part of the response are shown in Fig. 2, which reveals the presence of additional frequency components. The small

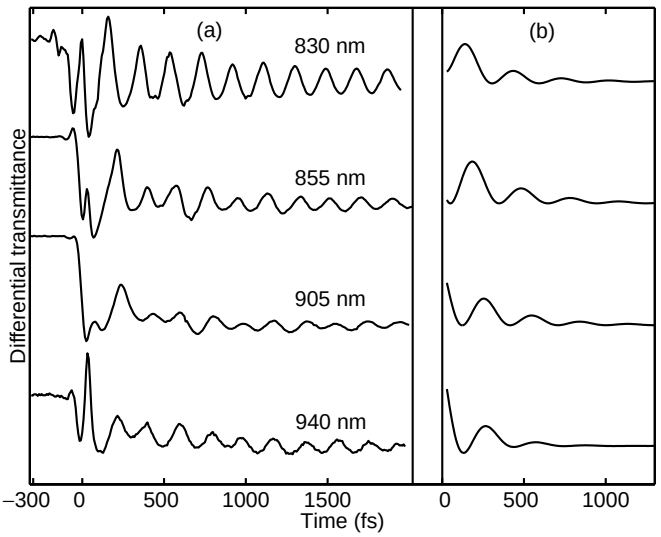

FIG. 1. (a) Time-resolved differential transmittance of $[Pt(en)_2][Pt(en)_2Br_2] \cdot (PF_6)_4$ following excitation of the IVCT band with 35 fs pulses centered at 800 nm. Measurements were taken at a series of detection wavelengths selected from a broadband femtosecond continuum. Structure at delay times during which the pump and probe pulses are overlapped (roughly ± 50 fs around $t = 0$) include contributions from cross phase modulation in the sample substrate that are not associated with the dynamics of the complex. (b) The sum of the low-frequency component and the zero-frequency component extracted by LPSVD analysis of each trace in part (a), showing the excited state contributions to the response and the systematic phase shift of the wave packet oscillation with detection wavelength.

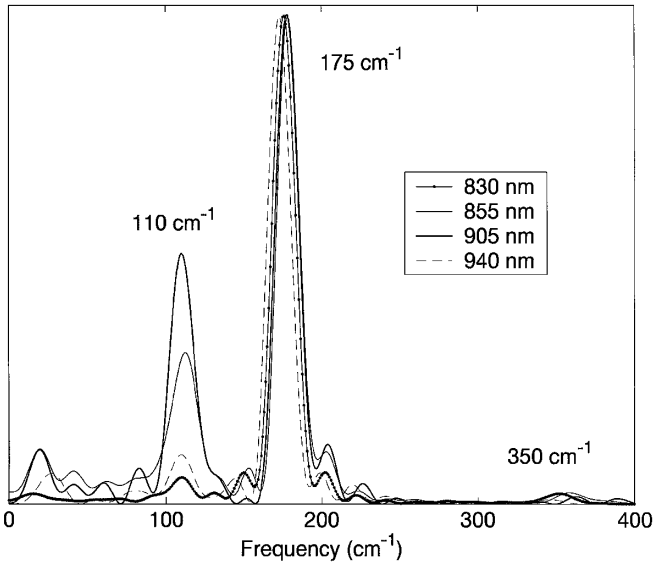

FIG. 2. Fourier power spectra of the oscillatory part of the data traces in Fig. 1(a).

peak at $\sim$350 cm^{-1} also corresponds to a feature in the cw Raman spectrum of $[Pt(en)_2][Pt(en)_2Br_2] \cdot (PF_6)_4$ [9], and can be identified as the second harmonic of the fundamental mode at 175 cm^{-1}. (Measurements taken in the degenerate pump-probe configuration, which provides a somewhat higher time resolution, show an additional component at $\sim$515 cm^{-1}, corresponding to the Raman third harmonic [10].) In contrast, the low-frequency Fourier component detected at $\sim$110 cm^{-1} is absent from the cw Raman spectrum.

To model the formation and evolution of the induced absorbance as well as the time course of the vibrational modulation, the data were fit to a sum of exponentials and exponentially damped cosinusoids using both linear prediction/singular value decomposition (LPSVD) [11] and traditional nonlinear least squares methods. The two methods generally gave consistent results, and the resulting LPSVD parameters are shown in Table I. The fits reveal a zero-frequency component, corresponding to the exponential formation of the underlying induced absorption signal, with a time constant of $\sim$200 fs. The fits also confirm the presence of a strong, heavily damped, low frequency component near 110 cm^{-1}. This oscillatory component has an amplitude comparable to that of the underlying induced absorbance signal, and is seen to decay on a time scale that closely follows the formation time of the induced absorbance. The phase of this rapidly damped component shifts systematically with detection wavelength, changing by $\sim$180° between 830 and 940 nm.

The wave packet oscillations correspond to a modulation of the optical response resulting from the lattice motions that are induced by photoexcitation. In order to interpret the oscillatory response in terms of the detailed vibrational dynamics, the origin of the individual components must

TABLE I. Results of LPSVD fits to the wavelength-resolved differential transmittance measurements in Fig. 1(a). Zero-frequency LPSVD components correspond to exponential decays.

Detection wavelength	Frequency (cm^{-1})	τ (fs)	ϕ (deg)	Amplitude
830 nm	0	190	···	0.022
	115	280	155	0.016
	175	1300	65	0.021
	351	670	100	0.0051
855 nm	0	290	···	0.016
	107	290	112	0.011
	176	1600	−35	0.0045
	344	400	−89	0.0023
905 nm	0	290	···	0.028
	114	290	21	0.010
	171	1000	−69	0.0037
	356	400	145	0.0059
940 nm	0	190	···	0.032
	109	180	14	0.023
	167	1300	−2	0.0079
	344	400	−99	0.002

be identified. Since we expect electronic dephasing in this condensed phase system to be extremely fast, we can effectively characterize the observed oscillatory modulations following the pump pulse in terms of distinct contributions from the ground and excited electronic states. The large component at $\sim$175 cm^{-1} is consistent with a vibrational wave packet in the ground electronic state: its frequency is close to that of the $\sim$180 cm^{-1} chain-axis symmetric stretching mode identified by resonance Raman spectroscopy, and the observed picosecond damping time is consistent with the measured Raman linewidth [10]. Excitation of ground state wave packets corresponding to the symmetric stretch mode can be understood in terms of an impulsive stimulated Raman scattering mechanism [12,13]. As noted above, wave packet oscillations detected at $\sim$350 cm^{-1} and $\sim$515 cm^{-1} correspond to the second and third harmonics of the fundamental chain-axis symmetric stretching mode, allowing these components to be identified as higher-order vibrational coherences in the ground electronic state.

The dynamics associated with the formation of the self-trapped exciton occur in the excited electronic state. Following photoexcitation of the IVCT band, the system is expected to undergo a rapid transition to the localized self-trapped exciton state, driven by the strong electron-lattice interaction. The formation of the STE is evidenced by the appearance of its characteristic optical absorption, which corresponds to an optical transition from the STE surface to a higher-lying electronic state, and which is redshifted relative to the ground state IVCT absorption. In these experiments, we have clearly time resolved the formation of

this optical absorption, which corresponds to the ~200 fs exponential component. The vibrational motion associated with the formation of the STE is evident in the large amplitude, strongly damped low-frequency modulation at ~110 cm^{-1}. The decay time of the ~110 cm^{-1} oscillatory component closely parallels the formation time of the STE absorption, consistent with the oscillatory component corresponding to the lattice motion that carries the system to the self-trapped state.

The excited state dynamics are evident in Fig. 1(b), which shows the sum of the LPSVD components associated with the excited state (i.e., the strongly damped ~110 cm^{-1} oscillatory component and the zero-frequency exponential formation of the STE induced absorbance), as reconstructed from the LPSVD fit parameters in Table I. The evolution of the wave packet in the excited state is particularly evident in the dependence of the oscillation phase on detection wavelength. The shortest detection wavelength, 830 nm, falls within the spectrum of the pump pulse, and therefore includes contributions from the wave packet as it is initially prepared in the Franck-Condon region. The initial phase of the oscillation is ~180°, consistent with the observation of an induced absorbance (i.e., negative differential transmittance) signal originating from the excited state potential surface and terminating on a higher-lying potential surface. As the wave packet propagates in the excited state, this induced absorbance shifts to longer wavelengths, as reflected by the phase shift for successively longer detection wavelengths. At a detection wavelength of 940 nm, the oscillation has shifted ~180° out of phase relative to its value in the Franck-Condon region, indicating that the wave packet has reached its outer turning point in the excited state. The amplitude of the excited state wave packet oscillation damps rapidly with time as the system undergoes conversion to the self-trapped state. The exponential damping time corresponds to slightly less than one cycle of the 110 cm^{-1} (300 fs period) vibrational motion, indicating that the theoretically barrierless STE formation occurs rapidly, but still appears to require repeated lattice motions before reaching completion. The wavelength-resolved impulsive excitation measurements clearly distinguish between the relatively long-lived ground state vibrational coherence at 175 cm^{-1} and the 110 cm^{-1} excited state coherence that damps in concert with the excited-state trapping, allowing the vibrational dynamics associated with the self-trapping process to be clearly observed.

This work was supported by the donors of The Petroleum Research Fund, administered by the American Chemical Society, by the National Science Foundation, and by Washington State University. The work at Los Alamos was supported by the Division of Materials Science of the Office of Basic Science, U.S. Department of Energy.

*Corresponding author.
†Present address: Department of Chemistry, University of New Mexico, Albuquerque, NM 87131.

[1] D. Redfield and R. H. Bube, *Photoinduced Defects in Semiconductors* (Cambridge University Press, New York, 1996).
[2] K. S. Song and R. T. Williams, *Self-Trapped Excitons*, Springer Series in Solid-State Sciences Vol. 105 (Springer, New York, 1996), 2nd ed.
[3] R. J. H. Clark, Adv. Infrared Raman Spectrosc. **11**, 95 (1984); S. P. Love *et al.*, Phys. Rev. B **47**, 11 107 (1993), and references therein.
[4] J. T. Gammel *et al.*, Phys. Rev. B **45**, 6408 (1992); M. Suzuki and K. Nasu, *ibid.* **45**, 1605 (1992); A. Mishima and K. Nasu, *ibid.* **39**, 5758 (1989); **39**, 5763 (1989).
[5] S. Tomimoto *et al.*, Phys. Rev. Lett. **81**, 417 (1998); Y. Wada *et al.*, J. Lumin. **58**, 146 (1994); Y. Wada, K. Era, and M. Yamashita, Solid State Commun. **67**, 953 (1988); H. Tanino, W. W. Ruhle, and K. Takahashi, Phys. Rev. B **38**, 12 716 (1988).
[6] H. Ooi, M. Yamashita, and T. Kobayashi, Solid State Commun. **86**, 789 (1993); G. S. Kanner *et al.*, Phys. Rev. B **56**, 2501 (1997).
[7] Y.-X. Yan, E. B. Gamble, and K. A. Nelson, J. Chem. Phys. **83**, 5391 (1985); W. T. Pollard, S.-Y. Lee, and R. A. Mathies, J. Chem. Phys. **92**, 4012 (1990).
[8] J. A. Brozik *et al.*, Inorg. Chem. Acta **294**, 275 (1999).
[9] J. A. Brozik and A. P. Shreve (unpublished).
[10] S. L. Dexheimer *et al.*, J. Phys. Chem. (to be published).
[11] F. W. Wise *et al.*, IEEE J. Quantum Electron. **23**, 1116 (1987).
[12] L. Dhar, J. A. Rogers, and K. A. Nelson, Chem. Rev. **94**, 157 (1994); V. Romero-Rochin and J. A. Cina, Phys. Rev. A **50**, 763 (1994); S. L. Dexheimer *et al.*, Chem. Phys. Lett. **188**, 61 (1992); W. T. Pollard *et al.*, J. Phys. Chem. **96**, 6147 (1992).
[13] This mechanism, which may include resonant enhancement effects, may also introduce a more complicated dependence of the oscillation phase on the detection wavelength, as seen in the results in Table I [10,12].